Full-Rate Full-Diversity Complex-Field Space-Time Codes for Frequency- or Time-Selective Fading Channels *

Xiaoli Ma and *Georgios B. Giannakis*

Dept. of ECE, Univ. of Minnesota, Minneapolis, MN 55455, U.S.A.

Abstract

Multi-antenna systems allow for a significant increase in transmission rates of coherent wireless transmissions over Rayleigh fading channels. Various multi-antenna designs have been developed in recent years targeting either high-performance, or, high rate. In this paper, we design a layered space-time (ST) scheme equipped with linear complex field (LCF) coding, which enables full diversity with full rate, for any number of transmit- and receive-antennas through either flat or non-flat fading channels. Our theoretical claims are confirmed by simulations.

1 Introduction

Rapid increase of cellular service subscribers and wireless applications has stipulated tremendous research efforts in developing systems that support reliable high rate transmissions over wireless channels. However, these developments must cope with challenges such as multipath fading, as well as bandwidth, and power limitations. Multi-antenna systems on the other hand, allow for a significant increase in the capacity of coherent wireless links, when communicating over flat Rayleigh fading channels [3]. Various multi-antenna designs have been developed targeting either high-performance through space-time coding (STC), or, high rate through layered transmissions: VBLAST [13], DBLAST [2], or, threaded ST (TST) [4]. Recently, STC has been combined with LCF codes (see e.g., [6]) or other (e.g., trellis) codes to collect joint space and multipath diversity. VBLAST and DBLAST schemes have also been employed to improve transmission rates over frequency-selective channels [14]. However, none of these existing schemes achieves full diversity and full rate simultaneously.

In this paper, we design a layered space-time scheme equipped with linear complex field (LCF) coding, which enables full diversity and full rate (FDFR) not only for flat-fading channels, but also for frequency-, or, time-selective channels. When the number of transmit-antennas is $N_t = 2$ and the channels are flat fading, our design subsumes the design in [1] as a special case. We also delineate the performance achieved when low-complexity sub-optimal decoding is employed.

Notation: Upper (lower) bold face letters will be used for matrices (column vectors). Superscript $^{\mathcal{H}}$ will denote Hermitian, and ^{T} transpose. We will reserve $\otimes$ for the Kronecker product; diag$[\boldsymbol{x}]$ will stand for a diagonal matrix with $\boldsymbol{x}$ on its main diagonal; and $\mathbb{Z}(j)$ will denote the integer ring, with elements $p + jq$ with $p, q \in \mathbb{Z}$.

2 System Model

Consider the system in Figure 1 with N_t transmit- and N_r receive-antennae.

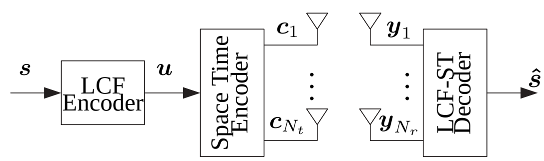

Figure 1: Equivalent MIMO model

The information bearing symbols $\{s(i)\}$ are drawn from a finite alphabet $\mathcal{A}_s$, and parsed into blocks of size $N \times 1$, so that $\boldsymbol{s} := [s(1), \ldots, s(N)]^T$. Every block $\boldsymbol{s}$ is split in sub-blocks (groups) $\{\boldsymbol{s}_g\}_{g=1}^{N_g}$, each of length N_{sub}; hence, $N = N_{sub} N_g$, where N_g is the number of groups. The LCF encoder $\{\boldsymbol{\Theta}_g\}_{g=1}^{N_g}$ per group is an $N_{sub} \times N_{sub}$ matrix with entries drawn from the complex field. Each sub-block $\boldsymbol{s}_g$ is coded linearly (via $\boldsymbol{\Theta}_g$) to obtain a coded sub-block as: $\boldsymbol{u}_g := \boldsymbol{\Theta}_g \boldsymbol{s}_g$ (hence the term LCF). We define an LCF coded group $\boldsymbol{u}_g$ as one *layer*, and N_g as the number of layers per information block. Concatenating $\{\boldsymbol{u}_g\}_{g=1}^{N_g}$ we obtain the $N \times 1$ block $\boldsymbol{u}$ which contains all the LCF coded symbols from $\boldsymbol{s}$.

Every $N \times 1$ block $\boldsymbol{u}$ is further mapped to N_t blocks $\{\mathbf{c}_\mu\}_{\mu=1}^{N_t}$ of size $P \times 1$, with each block $\boldsymbol{c}_\mu$ transmitted through the μth antenna. Each LCF coded symbol in $\boldsymbol{u}$ will be transmitted through one transmit antenna per time slot. This general transmitter structure subsumes VBLAST, DBLAST, and TST as special cases.

*The work in this paper was supported by the NSF Grant No. 0122431, and by the ARL/CTA Grant No. DAAD19-01-2-011.

Let $h_{\nu,\mu}(n)$ be the channel associated with the μth transmit-antenna, and the νth receive-antenna at the nth time-slot (or frequency bin). The nth sample at the receive-filter output of the νth antenna can be expressed as:

$$y_\nu(n) = \sum_{\mu=1}^{N_t} h_{\nu,\mu}(n) c_\mu(n) + w_\nu(n), \quad \forall \nu \in [1, N_r], \quad (1)$$

where $w_\nu(n)$ is complex additive white Gaussian noise (AWGN) at the νth receive-antenna with mean zero, and variance σ_w^2. Stacking the received samples from different antennas, we obtain the matrix counter part of (1) as

$$\boldsymbol{y}(n) = \boldsymbol{H}(n)\boldsymbol{c}(n) + \boldsymbol{w}(n), \ \ \forall n \in [1, P], \quad (2)$$

where the (ν, μ)th entry of $\boldsymbol{H}(n)$ is $h_{\nu,\mu}(n)$, and $\boldsymbol{c}(n) := [c_1(n), \ldots, c_{N_t}(n)]^T$. Before we pursue time- or frequency-selective fading channels, we consider flat-fading channels for which $h_{\mu,\nu}$ remains invariant during P time-slots.

3 FDFR over Flat-Fading Channels

For the flat channels dealt with in this section, we drop the index n.

3.1 LCF-STC codec

Since the channels are invariant over P symbol periods, the input-output relationship in (2) can be simplified as

$$\boldsymbol{Y} = \boldsymbol{H}\boldsymbol{C} + \boldsymbol{W}, \quad (3)$$

where $\boldsymbol{Y} := [\boldsymbol{y}(1), \ldots, \boldsymbol{y}(P)]$, and

$$\boldsymbol{C} := \begin{bmatrix} \boldsymbol{c}_1^T \\ \boldsymbol{c}_2^T \\ \vdots \\ \boldsymbol{c}_{N_t}^T \end{bmatrix} = \begin{bmatrix} c_1(1) & c_1(2) & \cdots & c_1(P) \\ c_2(1) & c_2(2) & \cdots & c_2(P) \\ \vdots & \vdots & & \vdots \\ c_{N_t}(1) & c_{N_t}(2) & \cdots & c_{N_t}(P) \end{bmatrix}. \quad (4)$$

To achieve the FDFR objective, we need to design both transmitter and receiver judiciously. Because of the page limitation, we will just outline the codec design here; see [8] for detailed exposition.

We select the block length $N = N_t^2$, and let each sub-block (and thus each layer) have length N_t, for a total of $N_g = N_t$ layers. Our FDFR encoder consists of two parts (see Fig. 1). The inner part called "ST encoder" is an ST mapping that we design as [7]:

$$\boldsymbol{C} = \begin{bmatrix} u_1(1) & u_{N_t}(2) & \cdots & u_2(N_t) \\ u_2(1) & u_1(2) & \cdots & u_3(N_t) \\ \vdots & \vdots & \cdots & \vdots \\ u_{N_t}(1) & u_{N_t-1}(2) & \cdots & u_1(N_t) \end{bmatrix}, \quad (5)$$

where $u_\mu(n)$ denotes the nth element of the μth layer. The outer part of the transmitter is termed "LCF encoder". Relying on the algebraic tools developed in [15, 5], we design the LCF encoders of the different groups as:

$$\boldsymbol{\Theta}_g = \beta^{g-1}\boldsymbol{\Theta}, \ \ \forall g \in [1, N_t], \quad (6)$$

where β is to be designed, and $\boldsymbol{\Theta}$ is a unitary Vandermonde matrix with generators $\{\alpha_i\}_{i=1}^{N_t}$ selected as in [15, 5].

With the inner and outer encoders in (5) and (6), after stacking the receive vectors $\boldsymbol{y}(n)$ into one vector, we have

$$\boldsymbol{y} = (\boldsymbol{I}_{N_t} \otimes \boldsymbol{H}) \begin{bmatrix} \boldsymbol{c}(1) \\ \vdots \\ \boldsymbol{c}(N_t) \end{bmatrix} + \boldsymbol{w}. \quad (7)$$

Furthermore, based on (5) and (6), we obtain

$$\boldsymbol{c}(n) = [(\boldsymbol{P}_n \boldsymbol{D}_\beta) \otimes \boldsymbol{\theta}_n^T]\boldsymbol{s},$$

where the permutation matrix $\boldsymbol{P}_n$, and the diagonal matrix $\boldsymbol{D}_\beta$ are defined, respectively, as

$$\boldsymbol{P}_n := \begin{bmatrix} \boldsymbol{0} & \boldsymbol{I}_{n-1} \\ \boldsymbol{I}_{N_t-n+1} & \boldsymbol{0} \end{bmatrix}, \ \boldsymbol{D}_\beta := \text{diag}[1, \beta, \ldots, \beta^{N_t-1}],$$

with $\boldsymbol{\theta}_n^T$ denoting the nth row of $\boldsymbol{\Theta}$.

By defining $\boldsymbol{\mathcal{H}} := \boldsymbol{I}_{N_t} \otimes \boldsymbol{H}$, and the unitary matrix

$$\boldsymbol{\Phi} := \begin{bmatrix} \boldsymbol{P}_1 \boldsymbol{D}_\beta \otimes \boldsymbol{\theta}_1^T \\ \vdots \\ \boldsymbol{P}_{N_t} \boldsymbol{D}_\beta \otimes \boldsymbol{\theta}_{N_t}^T \end{bmatrix},$$

we can rewrite (7) compactly as:

$$\boldsymbol{y} = \boldsymbol{\mathcal{H}}\boldsymbol{\Phi}\boldsymbol{s} + \boldsymbol{w}. \quad (8)$$

Maximum likelihood (ML) decoding can be used to detect $\boldsymbol{s}$ from $\boldsymbol{y}$ optimally, but with high complexity. Based on the structure of the system model in (8), sphere decoding (SD) or semi-definite programming algorithms can be used to achieve near-optimal performance. The decoding complexity depends on the length of $\boldsymbol{s}$, which here is $N = N_t^2$. When N_t is large, the decoding complexity is high even for near-ML decoders. To further reduce decoding complexity, we can resort to sub-optimal (nulling-cancelling based) decoding, which will be outlined next for our problem.

Based on (3) and (5), for the nth time slot, we have

$$\boldsymbol{y}(n) = \boldsymbol{H}_n \begin{bmatrix} u_1(n) \\ \vdots \\ u_{N_t}(n) \end{bmatrix} + \boldsymbol{w}_n, \quad (9)$$

where $\boldsymbol{H}_n := \boldsymbol{H}\boldsymbol{P}_n^T$. For a sub-optimal decoding alternative inspired by the nulling-cancelling (NC) algorithm of [13], we follow these major steps:

step 1 (nulling): Based on (9), perform QR decomposition for each n;

step 2 (sphere-decoding): Supposing the current layer is the gth layer, use SD to decode it;
step 3 (cancelling): Cancel the gth layer from all the other layers, then go to step 2) for $(g+1)$st layer.
Note that following QR-decomposition, SD is used to guarantee near-optimal performance per layer. We will analyze the performance for this case in the next subsection. Compared with the near-ML (SD) algorithm, the NC scheme has lower decoding complexity since in step 2), the SD is based on a layer of length $N_t < N_t^2$.

3.2 Performance analysis

To facilitate performance and mutual information analyses, we adopt the following assumption:
AS1) Channel taps $h_{\mu,\nu}$ are independently and identically Gaussian distributed with zero mean and unit variance.

We will summarize our major performance results for the design of Sec. 3.1 (see [8] for proofs).

Proposition 1: *For any constellation of $\boldsymbol{s}_g$ carved from $\mathbb{Z}(j)$, with the ST encoder in* (5), *there exists at least one pair of $(\boldsymbol{\Theta}, \beta)$ in* (6) *which enables full diversity ($N_t N_r$) for the ST transmission in* (3). *The design of $\boldsymbol{\Theta}$ is the same as that of [15, 5] for dimension N_t, and β can be selected as the N_tth root of any generator for $\boldsymbol{\Theta}$. The transmission rate is N_t symbols per channel use (pcu).*

Proposition 2 *Using nulling and cancelling as proposed in Section 3.1, when $N_r \geq N_t$ the design in* (5) *achieves diversity of order $N_t(N_r - N_t + g)$ for the gth decoded layer, when there is no error propagation. When error propagation is accounted for, the system performance is dominated by the worst layer, and the system diversity order becomes $N_t(N_r - N_t + 1)$, that of the worst layer's diversity.*

Simulated performance results can be found in [8].

3.3 Mutual information analysis

Suppose the information symbols are Gaussian distributed with zero mean and covariance matrix $\boldsymbol{R}_s = \mathcal{E}_s \boldsymbol{I}_N$, and define the average SNR as: $\gamma = \mathcal{E}_s / N_0$. The mutual information of our FDFR design is [c.f. (8)]:

$$\mathcal{C}_{FR} = \frac{1}{N_t} \log_2 \det \left(\boldsymbol{I}_N + \frac{\gamma}{N_t} \boldsymbol{\mathcal{H}}^{\mathcal{H}} \boldsymbol{\mathcal{H}} \right) \text{ bits pcu}$$
$$= \log_2 \det \left(\boldsymbol{I}_{N_t} + \frac{\gamma}{N_t} \boldsymbol{H}^{\mathcal{H}} \boldsymbol{H} \right) \text{ bits pcu.} \quad (10)$$

Since $\boldsymbol{H}^{\mathcal{H}} \boldsymbol{H}$ has at most $\min(N_t, N_r)$ non-zero eigenvalues (call them $\lambda_1, \ldots, \lambda_{\min(N_t, N_r)}$), the mutual information $\mathcal{C}_{FR}$ in (10) can be rewritten as

$$\mathcal{C}_{FR} = \sum_{\mu=1}^{\min(N_t,N_r)} \log_2 \left(1 + \frac{\gamma}{N_t} \lambda_\mu \right) \text{ bits pcu.}$$

At high SNR, the average (ergodic) capacity is

$$E[\mathcal{C}_{FR}] \approx \min(N_t, N_r) \log_2 \gamma + E \left[\sum_{\mu=1}^{\min(N_t,N_r)} \log_2 \left(\frac{\lambda_\mu}{N_t} \right) \right] \text{ bits pcu} \quad (11)$$

Eq. (11) shows that $E[\mathcal{C}_{FR}]$ increases linearly at high SNR with slope $\min(N_t, N_r)$ (see also [3]).

The mutual information for the LCF-STC design in [15], and for the ST orthogonal designs (ST-OD) in [10] is given, respectively, by

$$\mathcal{C}_{CF} = \frac{1}{N_t} \sum_{\mu=1}^{N_t} \log_2 \left(1 + \gamma \sum_{\nu=1}^{N_r} |h_{\mu,\nu}|^2 \right) \text{ bits pcu,}$$
$$\mathcal{C}_{OD} = R_{od} \log_2 \left(1 + \frac{\gamma}{N_t} \sum_{\mu=1}^{N_t} \sum_{\nu=1}^{N_r} |h_{\mu,\nu}|^2 \right) \text{ bits pcu,} \quad (12)$$

where R_{od} denotes the rate for ST-OD.

Comparing the mutual information of the aforementioned ST schemes, we have proved that [8]

$$\mathcal{C}_{FR} \geq \mathcal{C}_{OD} / R_{od} > \mathcal{C}_{CF}, \quad (13)$$

where the first equality holds if and only if $\min(N_t, N_r) = 1$. Closed form expressions of the outage pdf of $\mathcal{C}_{FR}$ in (10) can be computed in some cases (see e.g., [12]). Furthermore, we observe that for fixed $N_t > 1$ and fixed γ, the difference between $\mathcal{C}_{FR}$ and $\mathcal{C}_{OD}/R_{od}$ increases as N_r increases.

Fig. 2 depicts the cumulative distribution function (cdf) of the capacity in (10) when $N_t = 2$, and $\gamma = 10$ dB. When $N_r = 1$, $\mathcal{C}_{FR}$ is the same as $\mathcal{C}_{OD}$. This result coincides with that of [1]. As N_r increases, the gap between $\mathcal{C}_{FR}$ and $\mathcal{C}_{OD}$ (or $\mathcal{C}_{CF}$) increases. In Fig. 3, we plot the outage probability, $P(\mathcal{C}_{FR} < R)$ with $R = 4$ bits pcu. We observe that FDFR-STC has lower outage probability for any SNR, and when N_r increases, the diversity order increases and the gap of performance between our FDFR and ST-OD (or LCF-STC) increases accordingly.

4 FDFR over Non-Flat Channels

Suppose the degrees of freedom in time (delay lag) or frequency (Doppler) domain are $L+1$; i.e., if the channel is frequency-selective (FIR of order L), then it has $L+1$ independent taps; and if the channel is time-selective, then it has $L+1$ bases (see [8] and references therein). It is not difficult to show that the model (2) can describe, on a per sub-carrier basis, MIMO-OFDM transmissions over frequency-selective channels. At the same time, it can also model MIMO transmissions over time-selective channels.

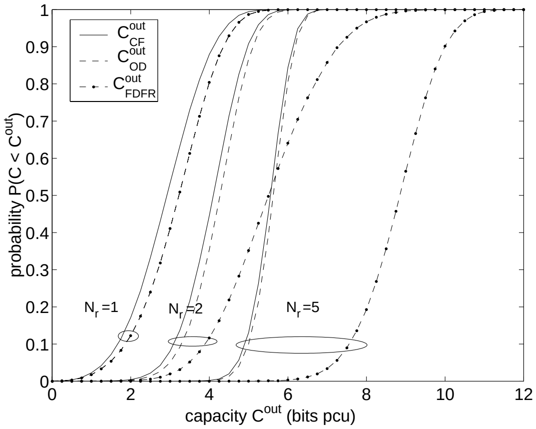

Figure 2: Capacity CDF

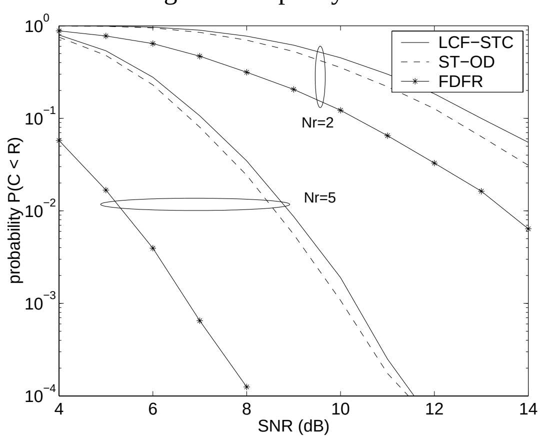

Figure 3: Outage probability with $R = 4$ bits pcu

Now let us stack the received blocks $\boldsymbol{y}(n)$ from N time-slots (or subcarriers/frequency-bins) as

$$\boldsymbol{y} = \begin{bmatrix} \boldsymbol{H}(1) & & \\ & \ddots & \\ & & \boldsymbol{H}(N) \end{bmatrix} \begin{bmatrix} \boldsymbol{c}(1) \\ \vdots \\ \boldsymbol{c}(N) \end{bmatrix} + \begin{bmatrix} \boldsymbol{w}(1) \\ \vdots \\ \boldsymbol{w}(N) \end{bmatrix}. \quad (14)$$

The SD algorithm can then be employed to find the near-optimum estimate of the information block $\boldsymbol{s}$. Note that the block size is larger than the one for flat-fading channels, simply because $L > 0$.

On this more general model, we have established the following result on performance:

Proposition 3: *If each channel is frequency- (or time-)selective with $L+1$ taps (or bases), then to enable FDFR, the ST matrix can be designed as* (15) *shown at the top of the page. The LCF encoder depends on the pair $(\boldsymbol{\Theta}, \beta)$, where the generator of the $N_t(L+1) \times N_t(L+1)$ matrix $\boldsymbol{\Theta}$ and β are designed according to [15, 5]. If at the receiver, SD is used, then the maximum diversity $(N_t N_r(L+1))$ is achieved. If NC decoding is employed, then the system diversity is $(N_r - N_t + 1)N_t(L+1)$.*

The general proof of Proposition 3 is provided in [9]. For brevity and clarity, we will prove it here for $(N_t, L) = (2, 1)$. For notational convenience, we consider frequency-selective channels, and select $N = N_t(L+1)$. Note that if we collect samples per receive antenna, then (2) can be rewritten as

$$\boldsymbol{y}^{(\nu)} = \sum_{\mu=1}^{N_t} \boldsymbol{D}_h^{(\mu,\nu)} \boldsymbol{c}_\mu + \boldsymbol{w}^{(\nu)}, \quad (16)$$

where $\boldsymbol{D}_h^{(\mu,\nu)} := \text{diag}[\boldsymbol{F}_{L+1} \boldsymbol{h}^{(\mu,\nu)}]$, with $\boldsymbol{F}_{L+1}$ denoting the first $L+1$ columns of FFT matrix, and $\boldsymbol{h}^{(\mu,\nu)}$ standing for the $L+1$ taps of the (μ,ν)th channel. Using the property that $\boldsymbol{D}_h^{(\mu,\nu)} \boldsymbol{c}_\mu = \boldsymbol{D}_c^{(\mu)} \boldsymbol{F}_{L+1} \boldsymbol{h}^{(\mu,\nu)}$ with $\boldsymbol{D}_c^{(\mu)} = \text{diag}[\boldsymbol{c}_\mu]$, we obtain [c.f. (16)]

$$\boldsymbol{y}^{(\nu)} = \boldsymbol{\Lambda} \boldsymbol{h}^{(\nu)} + \boldsymbol{w}^{(\nu)}, \nu \in [1, N_r], \quad (17)$$

where $\boldsymbol{\Lambda} := [\boldsymbol{D}_c^{(1)} \boldsymbol{F}_{L+1} \cdots \boldsymbol{D}_c^{(N_t)} \boldsymbol{F}_{L+1}]$, and $\boldsymbol{h}^{(\nu)} = [(\boldsymbol{h}^{(1,\nu)})^T \cdots (\boldsymbol{h}^{(N_t,\nu)})^T]^T$. Based on pairwise-error probability analysis (see e.g., [10]), we know that to achieve full diversity $(N_t N_r(L+1))$, the matrix $\boldsymbol{\Lambda}$ has to be full rank $(N_t(L+1))$ for any non-zero error pattern $\boldsymbol{s} - \boldsymbol{s}' \neq \boldsymbol{0}$.

When $(N_t, L) = (2, 1)$ and $N = 4$, we can write matrix $\boldsymbol{\Lambda}$ as:

$$\boldsymbol{\Lambda} = \begin{bmatrix} c_1(1) & c_1(1) & c_2(1) & c_2(1) \\ c_1(2) & jc_1(2) & c_2(2) & jc_2(2) \\ c_1(3) & -c_1(3) & c_2(3) & -c_2(3) \\ c_1(4) & -jc_1(4) & c_2(4) & -jc_2(4) \end{bmatrix}. \quad (18)$$

Considering the ST mapping in (15) and LCF encoding as

$$\boldsymbol{u}_1 = \boldsymbol{\Theta} \boldsymbol{s}_1, \;\; \boldsymbol{u}_2 = \beta \boldsymbol{\Theta} \boldsymbol{s}_2,$$

we obtain that the determinant of $\boldsymbol{\Lambda}$ in terms of $\boldsymbol{s}_g$ and $(\boldsymbol{\Theta}, \beta)$ is given by:

$$\begin{aligned} \det\,(\boldsymbol{\Lambda}) = 2j \Bigg(-2 \prod_{n=1}^{4} \boldsymbol{\theta}_n^T \boldsymbol{s}_1 + \beta^2 \Bigg(\prod_{n=1}^{2} \boldsymbol{\theta}_n^T \boldsymbol{s}_1 \prod_{n=3}^{4} \boldsymbol{\theta}_n^T \boldsymbol{s}_2 \\ + \; (\boldsymbol{\theta}_1^T \boldsymbol{s}_1)(\boldsymbol{\theta}_4^T \boldsymbol{s}_1) \prod_{n=2}^{3} \boldsymbol{\theta}_n^T \boldsymbol{s}_2 + (\boldsymbol{\theta}_1^T \boldsymbol{s}_2)(\boldsymbol{\theta}_4^T \boldsymbol{s}_2) \prod_{n=2}^{3} \boldsymbol{\theta}_n^T \boldsymbol{s}_1 \\ + \; \prod_{n=1}^{2} \boldsymbol{\theta}_n^T \boldsymbol{s}_2 \prod_{n=3}^{4} \boldsymbol{\theta}_n^T \boldsymbol{s}_1 \Bigg) - 2\beta^4 \prod_{n=1}^{4} \boldsymbol{\theta}_n^T \boldsymbol{s}_2 \Bigg). \quad (19) \end{aligned}$$

Note that (19) is a polynomial in β^{N_t} with coefficients in $\mathbb{Z}(j)$ if $\boldsymbol{s}_g \in \mathbb{Z}(j)$. To guarantee the coefficients of $\det(\boldsymbol{\Lambda})$ in β^{N_t} are zero simultaneously, when $\boldsymbol{s} - \boldsymbol{s}' \neq \boldsymbol{0}$, we design $\boldsymbol{\Theta}$ according to [5, 15, 8]. In this special case, we select $\boldsymbol{\Theta}$ as:

$$\boldsymbol{\Theta} = \frac{1}{2} \begin{bmatrix} 1 & e^{j\frac{\pi}{8}} & e^{j\frac{2\pi}{8}} & e^{j\frac{3\pi}{8}} \\ 1 & e^{j\frac{5\pi}{8}} & e^{j\frac{10\pi}{8}} & e^{j\frac{15\pi}{8}} \\ 1 & e^{j\frac{9\pi}{8}} & e^{j\frac{18\pi}{8}} & e^{j\frac{27\pi}{8}} \\ 1 & e^{j\frac{13\pi}{8}} & e^{j\frac{26\pi}{8}} & e^{j\frac{39\pi}{8}} \end{bmatrix}. \quad (20)$$

$$
\boldsymbol{C} = \begin{bmatrix} u_1(1) & \cdots & u_2(N_t) & u_1(N_t+1) & \cdots & u_2(2N_t) & \cdots & u_2(N) \\ u_2(1) & \cdots & u_3(N_t) & u_2(N_t+1) & \cdots & u_3(2N_t) & \cdots & u_3(N) \\ \vdots & \cdots & \vdots & \vdots & \cdots & \vdots & & \\ u_{N_t}(1) & \cdots & u_1(N_t) & u_{N_t}(N_t+1) & \cdots & u_1(2N_t) & \cdots & u_1(N) \end{bmatrix} \tag{15}
$$

Given $\boldsymbol{\Theta}$, we can view $\det(\boldsymbol{\Lambda})$ as a polynomial in β^{N_t} with coefficients in $\mathbb{Z}(j)$. Using the method in [5, 15, 8], we can find β^{N_t} such that $\forall \boldsymbol{s} - \boldsymbol{s}' \neq \boldsymbol{0}$, $\det(\boldsymbol{\Lambda}) \neq 0$. ■

We compare our FDFR with an existing scheme [6], for $(N_t, N_r, L) = (2, 2, 1)$. To maintain transmission rate $R = 4$ bits pcu, we use QPSK for our FDFR scheme, and 16QAM for the GSTF in [6] (note that the rate deduction due to the cyclic prefix is not accounted for here). SD algorithm is used for GSTF and both SD and NC are tested for our FDFR scheme. Fig. 4 depicts the simulated performance. Reading from the bit-error rate (BER) curves' slope, we validate our theoretical results in Proposition 3. Because our FDFR can afford smaller constellation sizes, it outperforms GSTF by more than 8 dB. But even with NC decoding, our FDFR achieves performance similar to GSTF. The price we pay here is decoding complexity.

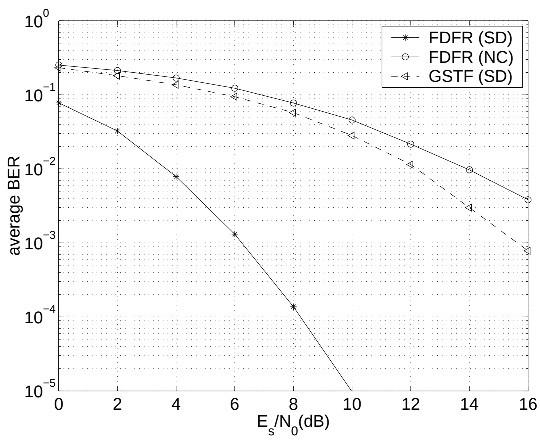

Figure 4: FDFR over frequency-selective channels

References

[1] M. O. Damen, A. Tewfik, and J.-C. Belflore, "A construction of a space-time code based on number theory," *IEEE Trans. on Infor. Theory*, pp. 753–760, March 2002.

[2] G. J. Foschini, "Layered space-time architecture for wireless communication in fading environments when using multiple antennas," *Bell Labs. Tech. Journal*, vol. 2, Autumn 1996.

[3] G. J. Foschini and M. J. Gans, "On limits of wireless communication in a fading environment when using multiple antennas," *Wireless Personal Communications*, pp. 311–335, Mar. 1998.

[4] H. E. Gamal and A. R. Hammons Jr., "A new approach to layered space-time coding and signal processing," *IEEE Trans. on Infor. Theory*, pp. 2321–2334, Sep. 2001.

[5] X. Giraud, E. Boutillon, J. C. Belfiore, "Algebraic tools to build modulation schemes for fading channels," *IEEE Trans. on Infor. Theory*, pp. 938–952, May 1997.

[6] Z. Liu, Y. Xin, and G. B. Giannakis, "Space-Time-Frequency Coded OFDM over Frequency-Selective Fading Channels," *IEEE Trans. on Signal Proc.*, pp. 2465–2476, Oct. 2002.

[7] X. Ma, and G. B. Giannakis, "Layered space-time complex field coding: full-diversity with full-rate, and tradeoffs," *Proc. of the 2nd Sensor Array and Multichannel SP Workshop*, pp. 442–446, Rosslyn, VA, August 4–6, 2002.

[8] X. Ma, and G. B. Giannakis, "Complex field coded MIMO systems: performance, rate, and tradeoffs," *Wireless Comm. and Mobile Computing*, Nov./Dec. 2002.

[9] X. Ma, and G. B. Giannakis, "Full-Rate Full-Diversity Complex-Field Space-Time Codes for Frequency- or Time-Selective Fading Channels," *IEEE Trans. on Infor. Theory*, submitted 2002.

[10] V. Tarokh, N. Seshadri, and A. R. Calderbank, "Space-time codes for high data rate wireless communication: performance criterion and code construction," *IEEE Trans. on Infor. Theory*, pp. 744–765, Mar. 1998.

[11] V. Tarokh, A. Naguib, N. Seshadri, and A. R. Calderbank, "Combined array processing and space-time coding," *IEEE Trans. on Infor. Theory*, pp. 1121–1128, May 1999.

[12] Z. Wang and G. B. Giannakis, "Outage Mutual Information for MIMO Space-Time Channels," *Proc. of 40th Allerton Conf.*, Monticello, IL, Oct. 2-4, 2002.

[13] P. W. Wolniansky, G. J. Foschini, G. D. Golden, and R. A. Vlenzuela, "V-BLAST: An architecture for realizing very high data rates over the rich-scattering wireless channel," *Proc. of URSI International Symposium Signals, Systems, and Electronics*, Italy, Sept. 1998.

[14] Y. Xin, and G. B. Giannakis, "High-Rate Space-Time Layered OFDM," *IEEE Comm. Letters*, pp. 187–189, May 2002.

[15] Y. Xin, Z. Wang, and G. B. Giannakis, "Space-time diversity systems based on linear constellation precoding," *IEEE Trans. on Wireless Communications*, 2002 (to appear); see also *Proc. of GLOBECOM*, pp. 455-459, San Antonio, TX, Nov. 25–27, 2001.

[16] L. Zheng and D. Tse, "Optimal diversity-multiplexing tradeoff in multi-antenna channels," *Proc. of the 39th Allerton Conference on Communication, Control and Computing*, pp. 835–844, Monticello, IL, Oct. 2001.